Theoretical Study on the $NO_2 + NO_2^-$ Electron Transfer Reaction

ZHOU, Zheng-Yu*,[a,b](周正宇)　　GAO, Hong-Wei[c](高洪伟)　　XING, Yu-Mei[a](邢玉梅)
GUO, Li[a](郭丽)　　QU, Yu-Hui[a](曲玉辉)

[a] *Department of Chemistry, Qufu Normal University, Shandong, Qufu 273165, China*
[b] *State Key Laboratory of Crystal Materials, Shandong University, Shandong, Jinan 250100, China*
[c] *State Key Laboratory for Structural Chemistry of Unstable & Stable Species, Institute of Chemistry,*
　Chinese Academy of Sciences, Beijing 100080, China

The $NO_2 + NO_2^-$ electron transfer reaction was studied with DFT-B3LYP method at 6-311 + G* basis set level for the eight selected structures: four species favor the structure of "head to head". The geometry of transition state was obtained by the linear coordinate method. Three parameters, non-adiabatic activation energy (E_{ad}), coupling matrix element (H_{if}) and reorganization energy (λ) for electron transfer reaction can be calculated. According to the reorganization energy of the ET reaction, the values obtained from George-Griffith-Marcus (GGM) method (the contribution only from diagonal elements of force constant matrix) are larger than those obtained from Hessian matrix method (including the contribution from both diagonal and off-diagonal elements), which suggests that the coupling interactions between different vibrational modes are important to the inner-sphere reorganization energy for the ET reactions in gaseous phase. The value of rate constant was obtained by using above three activation parameters.

Keywords　electron transfer reaction, density functional theory, activation energy, transition state

Introduction

The relevant structure, spectroscopic and thermodynamic properties of NO_2/NO_2^- electron transfer reaction has been of widespread interest in the study of the chemical processes, biochemical processes and living science, and a number of theoretical and experimental studies have been performed on it.[1-7] It is important to study the nature of the transition state and the paths of electron transfer and especially the influences of environmental factors and molecular properties on the electron transfer rate. In general, for the following type of electron exchange reaction in the gas phase

$$NO_2 + NO_2^- = NO_2^- + NO_2 \qquad (1)$$

the dependence of the electron transfer rate (k) on certain parameters can be expressed as

$$k = \kappa_{el} \nu_N \exp(-E_{ad}/RT) \qquad (2)$$

where κ_{el} denotes the electronic transmission factor, ν_N the effective frequency, E_{ad} the activation energy, R the thermodynamic constant, and T the thermodynamic temperature. These parameters and their effect on the electron transfer rate have been extensively studied using various methods.[7-12] According to the Landau-Zener model,

$$k = \frac{2H_{if}^2}{h}\left(\frac{\pi^3}{\lambda RT}\right)^{1/2}\exp(-E_{ad}/RT) \qquad (3)$$

where H_{if} denotes the electron coupling matrix, h Planck's constant, and λ the reorganization energy. For the convenience of calculations, it is assumed that in a reaction the reactants diffuse toward each other to form "precursor complex" from which they react. Reaction then leads to a "successor complex" and thence by diffusion to the separated products. In the reaction process, the important species is the precursor complex, as its structure and relevant properties directly affect not only

the electron transfer mechanism but also its rate constant. In the absence of available experimental data, italics and density functional theory (DFT) calculations have played an important role in providing relevant information and in helping to elucidate the fundamental aspects regarding the precursor complex, the successor complex, the transition state and its structure reorganization in the ET reaction process.

The B3LYP (Beckes Three Parameter Hybrid Method using the LYP Correlation Functional) method[13,14] of density functional theory (DFT) was used to investigate the process of reaction (1). The equilibrium geometry of the precursor complex was computed and information about the nature of the interaction in the complex was obtained. In order to discuss the reaction mechanism, the geometries of the transition state were also analyzed. Additionally, three parameters, the coupling matrix element, the non-adiabatic activation energy and the reorganization energy for this ET reaction were calculated. Finally, according to Eq. (3), the rate constant of ET reaction was derived.

Calculation

All calculations were performed using the Gaussian-94 program package. As a new quantum chemical method, DFT has been exponentially used in inorganic and organo-metallic chemistry in the past few years with great success.[15,16] Unlike the Hartree-Fork theory, DFT recovers electron correlation in the self-consistent Kohn-Sham procedure through the functions of electron density and gives good descriptions for systems, which require sophisticated treatments of electron correlation in the conventional *ab initio* approach. Hence not only is it a cost effective method, but also a reliable one. The results obtained from the DFT method are generally in good agreement with the experimental and the MP2 calculated values. In this paper, the geometrical optimizations and electronic structure calculations for the isolated species and the precursor complex were performed with the DFT/B3LYP method using the 6-311 + G* basis set.

Results and discussion

Equilibrium geometry of NO_2 *and* NO_2^-

Before the structures of the precursor complex and

the activation complex of the ET system are discussed, it is useful to test the applicability of the italics calculation level to this system. The calculations on the isolated species, NO_2 ($\widetilde{X}^2 A_1$) and NO_2^- ($\widetilde{X}^1 A_1$), were performed at the level of B3LYP, using the 6-311 + G* basis set. The optimized structures, energies and vibrational frequencies of NO_2 and NO_2^- are summarized in Table 1. By comparing the calculated and experimental values for the spectroscopic constants, some trends in the dependence of the quality of the results on the level of theory used can be identified. It may be noted that, even at the MP2 level, larger deviations were found than with B3LYP method. The worst agreement between calculated and experimental results was found using HF/6-311 + G*. The inclusion of electron correlation correction may decrease the errors in the internuclear distances and bond angles. The HF/6-311 + G* is the same as the MP2/6-311 + G*, and the results indicate that significant accuracy is achieved in comparison with the experimental values. Comparison of the experimental r_e and a value with those calculated at the B3LYP/6-311 + G* level results in an error in bond distance of about 0.0494%—0.632% and in bond angle of about 0.3892%—0.6072%. The mean absolute deviations between non-NO and NO stretching frequencies of NO_2 species and the raw B3LYP, MP2 and scaled HF results are 49.34, 313.70 and 202.03 cm^{-1}, respectively, while those of NO_2^- are 42.25, 75.51 and 230.47 cm^{-1}, respectively. It indicates that the raw B3LYP calculations approximate the observed fundamental frequencies, and it is much better than the MP2 and HF results. Therefore, the high level of conformity between the observed and calculated spectral features indicates that scaled B3LYP, is a more straightforward and practical approach to deduce the observed fundamental vibrational frequencies for many molecules whose vibrational spectra are not well understood. The analysis has fully confirmed that this electron correlation method is applicable in investigating the structure and spectroscopic properties of these small species containing nitrogen.

Equilibrium geometry of the precursor complexes

Formation of the precursor complex from the isolated redox species is the first stage of the ET reaction. The geometrical configuration of the precursor complex influences directly not only the activation energy of reaction

Table 1   Calculated bond distance, bond angle and spectroscopic properties for NO_2 and NO_2^-

Species	Method	r_e ($\times 10^{-1}$ nm)	A (degree)	ω (cm^{-1})		
NO_2	Exp.	1.19389[3]	133.857[3]	$\omega_1^0 = 1325.33$[1]	$\omega_2^0 = 750.14$[1]	$\omega_3^0 = 1633.86$[1]
	HF/6-311 + G*	1.156	136.3935	$\omega_1^0 = 1604.4808$	$\omega_2^0 = 848.3366$	$\omega_3^0 = 1862.6093$
	MP2/6-311 + G*	1.2026	133.939	$\omega_1^0 = 1378.8469$	$\omega_2^0 = 772.9799$	$\omega_3^0 = 2498.6236$
	B3LYP/6-311 + G*	1.1933	134.378	$\omega_1^0 = 1391.1199$	$\omega_2^0 = 764.6376$	$\omega_3^0 = 1701.5807$
NO_2^-	Exp.	1.25[3]	117.5[3]	$\omega_1^0 = 1284$[2]	$\omega_2^0 = 776$[2]	$\omega_3^0 = 1244$[2]
	HF/6-311 + G*	1.2192	117.4233	$\omega_1^0 = 1575.2652$	$\omega_2^0 = 900.6980$	$\omega_3^0 = 1519.4456$
	MP2/6-311 + G*	1.2643	116.3184	$\omega_1^0 = 1401.0708$	$\omega_2^0 = 802.7566$	$\omega_3^0 = 1326.6978$
	B3LYP/6-311 + G*	1.2579	116.7865	$\omega_1^0 = 1334.1717$	$\omega_2^0 = 799.2854$	$\omega_3^0 = 1297.2803$

but also the electron transfer coupling matrix element and the electron transfer rate. Thus it is very important to find various possible geometrical configurations for the precursor complex. For the ET reaction between NO_2 and NO_2^-, three possible structures of the precursor state have been considered when two isolated species contact (a) two nitrogen atoms have the structure of "head to head"; (b) four oxygen atoms have the structure of "head to head"; (c) a nitrogen atom contacts an oxygen atom to take on the "cross type" structure; (d) an oxygen atom contacts an oxygen atom to take on the "cross type" structure; (e) two oxygen atoms contact two oxygen atoms in different plane, but two nitrogen atoms in different direction; (f) an oxygen atom contacts an oxygen atom to take in different plane; (g) a nitrogen atom and two oxygen atoms contact a nitrogen atom and two oxygen atoms in different plane; (h) an oxygen atom contacts an oxygen atom in different plane. According to the structures in Fig. 1, the geometry optimization was performed. The results show that there is no stable position with the distance of the center of two-molecule decreasing for **T5**, **T6**, **T7** and **T8**. That is to say, the potential energy curve versus the reaction coordinate has no minimum point, so the conclusion can be derived that no stable equilibrium geometry for these four orientations exists. Actually, from the analysis of the key orbital of the species NO_2 and NO_2^-, structures **T1**, **T2**, **T3**, **T4** are preferred because the overlap between the electron acceptor orbital (mainly the outer shell Π_3^2 of NO_2) and the electron donor orbital (mainly the outer shell Π_3^4 of NO_2^-) will be the largest. For simplicity, the later discussion will restrict to structure **T1**, **T2**, **T3** and **T4**.
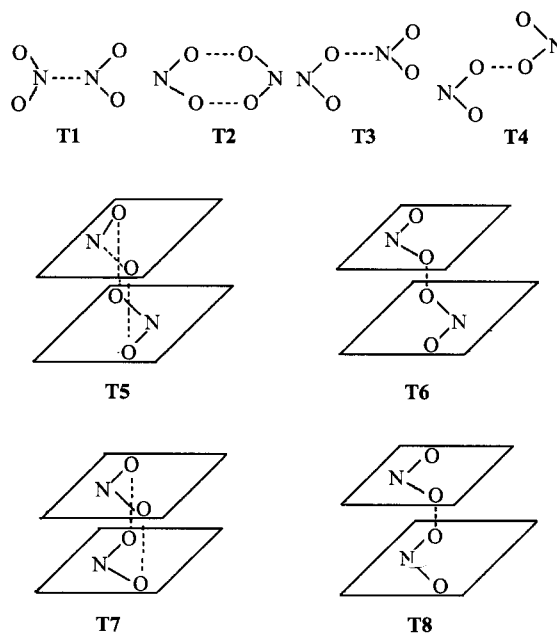
Fig. 1   Eight possible structures in precursor state for the ET reaction between NO_2 and NO_2^-.

In order to optimize the precursor complexes, the following three steps were used: (1) keeping the optimized geometries of NO_2 and NO_2^-, the contact distance R between two species is optimized; (2) fixing the optimized contact distance R and keeping r_- of NO_2^- equal to its optimized value in the isolated state, r_0 of NO_2 in the precursor complex is optimized; (3) keeping the optimized contact distance R and r_0', r_- of NO_2^- in the precursor complex is also optimized (r_-'). The geometry of the precursor complex can then be defined by three parameters R, r_0' and r_+'. In order to compare the stabilization of the different precursor complexes, the following equation is used

$$\Delta E = E_{NO_2} + E_{NO_2^-} - E_{ES} \qquad (4)$$

where ΔE is the stabilization energy of the precursor complex, E_{ES} the energy of the precursor complex and E_{NO_2}, and $E_{NO_2^-}$ the energies of NO_2 and NO_2^-, respectively. The larger the values of ΔE are, the more stable the complexes. Table 2 shows the values of structural parameters and ΔE of different systems in the precursor state. It can be seen that the bond length of one NO_2 fragment is slightly longer than that of isolated NO_2 molecule, while the NO_2^- fragment has a bond length much shorter than that of the isolated NO_2^-. The distances R range from 0.26 nm to 0.32 nm, yielding stabilization energies of about 0.5—0.9 eV where ΔE decreases in the order of T1 > T3 > T4 > T2. All these results indicate a relatively strong interaction between the acceptor and donor.

Transition state of reaction

The geometry of the transition state was calculated to study the mechanism of the ET reaction in NO_2 and NO_2^- systems. Once the linear coordinate is defined for the transition state of the reaction, the nuclear configuration parameter of the reacting system can be expressed as[17]

$$Q_i = RQ_i^R + (1 - R)Q_i^P \qquad (5)$$

where Q_i^R, Q_i^P and Q_i are the ith structural parameters of the reactant, product and the reacting system. According to the self-exchange model, $R = 0.5$ (the crossing point of two adiabatic potential energy surfaces) and the structural parameters R, r_0^* and r_+^*, used in the description of geometry of the transition state, can be obtained using Eq. (5). The geometry parameters are listed in Table 2. The results indicate that at the transition state, r_0^* is longer than r_0 while r_-^* is shorter than r_-. Actually, this state is in the preparation for converting into products.

Calculation of rate constant

From Table 2, it was observed that the values of E_a decrease in the order of T2 > T4 > T3 > T1, while for H_{if}, the order is T1 > T3 > T4 > T2. The activation energy of these reactions is relatively small, which suggests that the ET reaction rate constant should be large.

For the other parameter, reorganization energy (λ), two methods were used to compute it. According to the George-Griffth-Marcus (GGM) model, the force constant f_i ($i = z$ or $z + 1$) was obtained using the *ab initio* method in which only the diagonal elements were utilized.

$$f_i = \partial^2 U(q)/\partial q_{ii}^2 \qquad (6)$$

Table 2 Geometrical parameters, relevant energies, coupling matrix elements and rate constants for the reacting system in the precursor complex and transition state

Species	T1	T2	T3	T4
Coupling state	2-A1	2-B2	2-A'	2-A'
Precursor complex				
R (nm)	0.26287	0.31018	0.31445	0.28411
r_0 (nm)	0.12235	0.1225	0.12279	0.12283
r_- (nm)	0.12351	0.12387	0.12357	0.12287
a_0 (℃)	124.0532	124.568	124.1161	123.7379
a_- (℃)	121.3448	120.9849	121.098	123.7374
ΔE (eV)	0.8047	0.5503	0.6160	0.5765
Transition complex				
$r_0 = r_-$ (nm)	0.12256	0.12279	0.12221	0.12283
$a_0 = a_-$ (℃)	123.5442	123.7484	122.235	123.7379
E_a (kJ/mol)	28.24	32.56	29.58	30.49
H_{if} (kJ/mol)	2.81	2.70	2.79	2.74
k (s)	2.48×10^8	2.49×10^7	1.22×10^8	6.17×10^7

Then the inner-sphere reorganization energy of nitrogen dioxide systems was obtained using Eq. (7).

$$\lambda = 2n[f_z f_{z+1}/(f_z + f_{z+1})](\Delta q)^2 \qquad (7)$$

The results are listed in Table 3. For Hessian matrix method,[18] the total energy of a molecule, $U(q)$, can be represented by a Taylor series of the nuclear vibration modes of freedom around a given reference configuration, $\mathbf{q} = \{q_i\}$ as

$$U(\mathbf{q}) = \sum_{n=0}^{\infty} \frac{1}{n} [(\mathbf{q} - \mathbf{q_0}) \cdot \nabla]^n E(\mathbf{q_0}) \qquad (8)$$

where $\mathbf{q}$ is a vector containing the internal coordinates for the molecule. The vector $\mathbf{q_0}$ contains the internal coordinates for the molecule at the reference configuration. In the harmonic approximation, it can be obtained

$$U(\mathbf{q}) = U(\mathbf{q_0}) + {}^T G \Delta \mathbf{q} + \frac{1}{2} \Delta \mathbf{q}^T H \Delta \mathbf{q} + \cdots\cdots \qquad (9)$$

where superscript T indicates transposition of the vector. $\Delta \mathbf{q}$ is the displacement from the reference configuration given by

$$\Delta \mathbf{q} = \mathbf{q} - \mathbf{q_0} \qquad (10)$$

Since our method employs geometry-optimized structure at the DFT/B3LYP level, the gradient vanishes identically. From the Hessian matrix, the force constant matrix F is represented as

$$F = H \ (\mathbf{q} = \mathbf{q_{eq}}) \qquad (11)$$

For the above self-exchange ET reaction, a full geometry optimization is carried out for both the NO_2 and the NO_2^- systems and at the same time the force constant matrix F is obtained. The projected force constant f is determined by

$$f = \Delta \mathbf{q}^T F \Delta \mathbf{q} / |\Delta \mathbf{q}|^2 \qquad (12)$$

where $|\Delta \mathbf{q}|$ is the norm of the vector $\Delta \mathbf{q}$. This projected force constant also includes the off-diagonal elements in the Hessian matrix, $i.e.$, the coupling interactions between the different vibration modes, which were tradition-

ally omitted in earlier studies, are taken into account. For example, in the George-Griffith-Marcus equation, only the diagonal element of the inclusion of coupling interaction between different vibration modes via the off diagonal elements on inner-sphere λ will be also determined. According to the previous steps, the inner-sphere reorganization energy can be expressed as

$$\lambda = \bar{F} |\Delta \mathbf{q}| \qquad (13)$$

where $\bar{F}$ is the reduced force constants for the oxidized and reduced species respectively. For comparisons, it was also listed in Table 3.

Table 3   Reorganization energy for the reaction between NO_2 and NO_2^- system (kJ/mol)

Method	T1	T2	T3	T4
GGM	75.35	177.22	104.50	153.6
Hessian matrix	39.91	103.44	54.09	86.45

The results in Table 3 show that both of the sequences of the values obtained from GGM and Hessian Matrix methods are **T2 > T4 > T3 > T1**. This follows the trend of the activation energy. If we compare our method, which takes advantage of projected force constants, with the classical GGM treatment, which uses the diagonal elements of the force constant matrix only, it is found that λ obtained from the GGM scheme is larger. This discrepancy is related to the fact that the GGM treatment does not include the contribution from the non-diagonal elements of the force constant matrix that represents the coupling interaction between different vibrational modes, whereas the Hessian matrix method does. It clearly shows that the nondiagonal elements in the force constant matrix are very important in calculating λ and that the inner sphere reorganization energy resulting from the Hessian matrix method are more accurate. In the system of nitrogen dioxide, we consider that the Π electron prefers to move in the co-plane rather than no-plane. Particularly, when two isolated complexes of NO_2 and NO_2^- contact via the "head to head" structure (**T1** in Fig. 1) to form the large Π conjugated bond, the model of the electron transfer should be "through bond" but not "through space". This makes it easy for the electron to transfer and yields the relatively small reorganization energy. Subsequently, according to Eq. (3), rate con-

stants can be obtained. The results are listed in Table 2, and in this Table it can be seen that the rate constants of different reacting system increase in the same order as the activation energies and reorganization energies increase, namely **T2 > T4 > T3 > T1**.

Conclusion

The structures and properties of the ET system containing NO_2 and NO_2^- were studied in this paper at the B3LYP/6-311 + G* level. Geometry optimizations of the precursor complexes were performed and the results show that there are relatively strong interactions between acceptor and donor. The geometry of the transition state using the linear coordinate method was also obtained as the reaction mechanism of electron transfer was. In order to derive the rate constant, we discussed the three relevant activation parameters (H_{if}, E_a, λ) of the different reacting systems. Finally we obtain the rate constants, the sequence of those was **T2 > T4 > T3 > T1**.

References

1   Lafferty, W. J.; Sams, R. L. *J. Mol. Spectrosc.* **1977**, 66, 478.

2   Jacox, M. E. *J. Phys. Chem. Ref. Data* **1984**, 18, 945.

3   Kent, M.; Ervin, J. H.; Lineberger, W. C. *J. Phys.* *Chem.* **1988**, 92, 5405.

4   Zhou, Z. Y.; Xu, J.; Zhang, C. S; Zhou, X. M.; Du, D. M.; Zhang, K. Z. *J. Mol. Struct.* (*Theochem.*) **1999**, 469, 1.

5   (a) Hush, N. S. *Trans. Faraday Soc.* **1961**, 57, 557.
     (b) Hush, N. S. *Electrochim. Acta* **1968**, 13, 1005.

6   Zhou, Z. Y.; Khan, S. U. M. *J. Phys. Chem.* **1989**, 93, 5292.

7   Khan, S. U. M.; Zhou, Z. Y. *J. Chem. Phys.* **1990**, 93, 8808.

8   Cannon, R. D. *Electron Transfer Reaction*, Butterworths, London, **1980**.

9   Sutin, N. *Progress in Inorganic Chemistry*, Vol. 30, Ed.: Lippard, S. J., Wiley, New York, **1982**.

10   Newton, M. D. *Int. J. Quantum Chem.*, *Quantum Chem. Symp.* **1980**, 14, 363.

11   Bockris, J. O. M.; Khan, S. U. M. *Quantum Electrochemistry*, Plenum Press, New York, **1979**.

12   Bu, Y. X.; Deng, C. H. *J. Phys. Chem.* **1996**, 100, 18093.

13   Lee, C.; Yang, W.; Parr, R. G. *Phys. Rev. B* **1988**, 37, 785.

14   Becke, A. D. *Phys. Rev. A* **1988**, 38, 3098.

15   Zhou, X. F.; Christine, J. M.; Liu, R. F. *Vib. Spectrosc.* **1996**, 12, 53.

16   Jacek, K.; Uchimaru, T. *J. Phys. Chem. A* **1998**, 102, 2439.

17   Li, X. Y.; Xu, X. J.; He, F. C. *Acta Chim. Sinica* **1998**, 56, 251.

18   Jaxobsin, S.; Mikkelsen, K. V.; Pedersen, S. U. *J. Phys. Chem.* **1996**, 100, 7411.